Chemical Wave Plumes

in a Supercritical Tube

by

Michael C. Rogers

A report submitted in conformity with the requirements

for the degree of Master of Science

Department of Physics

University of Toronto

Abstract

Propagating reaction-diffusion fronts are found in many autocatalytic reactions, such as the iodate oxidation of arsenous acid. This reaction has been studied extensively in quasi two-dimensional layers and capillary tubes in both horizontal and vertical orientations. In capillary tubes the iodate-arsenous acid reaction shows convective behavior when a dimensionless driving parameter that is proportional to the cube of the radius exceeds a critical value. The buoyancy force that drives convection is created primarily by the lower density of the solution left in the wake of the propagating front. This report details the distinguishing characteristics of chemically reactive plumes that form in vertically oriented supercritical tubes held at four different temperatures. Collapsing of thin front filaments is also discussed, along with an examination of the relationship between front speed and temperature in capillary tubes.

Acknowledgements

I thank my supervisor, Prof. Stephen Morris, for his insight, patience, and for the idea that became this project. I also thank the members of the Experimental Nonlinear Physics group for their assistance and support. Finally, I thank my friends for their distractions during this entire process.

Contents

List of Figures

List of Tables

Chapter 1

Introduction

1.1 Chemical Waves

When the kinetic behavior of chemical reactions is nonlinear, fascinating spatiotemporal phenomena can occur. Such phenomena include: stationary spatial patterns, periodic and chaotic oscillations of chemical concentration, and chemically reactive traveling waves. A nonlinear chemical system that exhibits traveling waves is the focus of this report.

Traveling chemical waves are the result of the coupling of chemical reaction with diffusion, provided that the reaction exhibits some appropriate form of kinetic feedback such as autocatalysis [1]. Chemical waves occur in two distinctly different forms: propagating pulses and propagating fronts.

The most famous chemical waves are the propagating pulses found in the Belousov-Zhabotinsky (BZ) reaction. In the BZ reaction, as a pulse of reactivity passes through a point, the intermediates of the chemical reaction undergo a departure from their original concentration, only to return to their original state as the pulse passes by. During this process only a small amount of the reactants are depleted, therefore the pulse effectively regenerates the original kinetic state of the solution that it leaves in its wake [2].

Like a propagating pulse of chemical reactivity, as a propagating front passes through a point the chemical species involved in the reaction undergo a concentration

excursion. However, unlike propagating pulses, the solution left in the wake of the front is left in a new kinetic state. Such behavior was first observed in the iodate oxidation of arsenous acid (IAA reaction) in 1955 by Epik and Shub [3]. However, serious study and interest in the propagating front behavior of the IAA reaction did not begin until many years later, when in 1981 research began on the IAA reaction in thin layers and narrow tubes [4].

1.2 The IAA Reaction

The propagating front in the IAA reaction consumes reaction mixture that is in a state where very little reaction has occurred and leaves in its wake a solution in a state of thermodynamic equilibrium. Heat is produced during the reaction, as it is slightly exothermic. In addition, there is also an isothermal density change due to the difference in partial molal volumes of the reactant and product solutions. The partial molal volume change causes the front to leave behind a product solution that is less dense than the reactant solution. The IAA reaction is conveniently described by two coupled reaction steps, each of which consumes a product in the other reaction step. The reactions are the Dushman reaction [6] (process A)

$$IO_3^- + 5\ I^- + 6H^+ = 3I_2 + 3H_2O \tag{A}$$

and the Roebuck reaction [7] (process B)

$$H_3AsO_3 + I_2 + H_2O = 2I^- + H_3AsO_4 + 2H^+. \tag{B}$$

The rates of these reaction steps are:

$$R_A = \frac{-1}{5}\frac{d[I^-]}{dt} = (k_1 + k_2[I^-])[IO_3^-][H^+]^2[I^-] \tag{3.1}$$

$$R_B = \frac{-d[I_2]}{dt} = \frac{k_3[I_2][H_3AsO_3]}{[I^-][H^+]}. \tag{3.2}$$

The rate constants k_1, k_2, and k_3 have been determined [1] to be: $k_1 = 4.5 \times 10^{-2}\,M^{-3}\,s^{-1}$, $k_2 = 1.0 \times 10^{-8}\,M^{-4}\,s^{-1}$, and $k_3 = 3.2 \times 10^{-2}\,M\,s^{-1}$.

In the IAA reaction, when initial arsenous acid concentration is in stoichiometric excess to iodate ($[As(III)]_0 > 3[IO_3^-]_0$) the net reaction is (A) + 3(B), or

$$IO_3^- + 3H_3AsO_3 = I^- + 3H_3AsO_4. \qquad\qquad (3.3)$$

The rate of process (A) depends on iodide concentration, and the iodine product from (A) is reduced by the faster process (B) to regenerate iodide. Thus, iodide concentration undergoes an autocatalytic increase until the iodate in solution is completely consumed. When starch indicator is present in these solutions the propagating front appears as a thin blue line, with clear solution both preceding and in the wake of the propagating front.

When iodate is in stoichiometric excess to arsenous acid ($[As(III)]_0 < 5/2[IO_3]_0$) the net reaction is 2(A) + 5(B), or

$$2IO_3^- + 5H_3AsO_3 + 2H^+ = I_2 + 5H_3AsO_4 + H_2O \qquad\qquad (3.4)$$

Once again, an autocatalytic production of iodide according to (A) + 3(B) occurs, however for this case it is limited by the amount of arsenous acid present, rather than by the amount of iodate. The iodide that accumulates is then oxidized to iodine by process (A) and the result is the net reaction (3.4) [2]. Starch indicator in these solutions causes the front and all of the solution that it has consumed to appear blue. When the initial reaction mixture contains $5/2[IO_3^-]_0 < [As(III)]_0 < 3[IO_3^-]_0$ the net reaction is described by an appropriate linear combination of (3.3) and (3.4).

1.3 Review of Past Experimental Results

Over the course of the last 20 years, a considerable amount of experimental and theoretical work has been done on the IAA reaction. This work has been carried out for the reaction in two geometries: thin layers and narrow tubes.

1.3.1 IAA Fronts in a Thin Horizontal Layer

In a thin, horizontal, essentially two-dimensional layer, the change in the density between the reactant and product in the IAA system does not aid in the transport of autocatalyst. Therefore, the reaction front motion is purely a reaction-diffusion process. Initial experiments [1,4,8] involving IAA in a thin horizontal layer primarily involved determining the front speed of the reaction as a function of changes in solution acidity, and as a function of the ratio the initial concentrations of arsenous acid and iodate.

The ratio of initial arsenous acid concentration to initial iodate concentration is defined as:

$$R = [H_3AsO_3]_0 / [IO3]_0. \tag{3.5}$$

Experiments were performed in temperature controlled petri dishes in which negatively biased platinum electrodes at the center of the dish were used to initiate the reduction of iodate to iodide and thus initiate the front. It was found that the speed of fronts in the excess iodate regime ($R < 3$) and in the excess arsenous acid ($R \geq 3$) regime behave very differently.

In the excess arsenous acid regime plots of front position as a function of time were linear. A linear dependence of wave velocity on iodate concentration, arsenous acid concentration, and hydrogen ion concentration was also observed. In the excess iodate regime, plots of wave position as a function of time were found to be exponential, where the velocity is a linear function of distance. It was also found that in this regime the velocity increases at any particular distance with increasing $[IO_3^-]$, $[H_3AsO_3]$, or $[H^+]$. In both [1] and [4] simple reaction-diffusion models were presented to explain the observed behavior.

The IAA reaction is autocatalytic in both iodide and hydrogen ion. While the majority of the work [1,4,5] done on the IAA reaction has used buffers to maintain the desired $[H^+]$ during the course of the reaction, there is one exception [8] where it was studied in an unbuffered solution, allowing for an opportunity to investigate reaction-diffusion behavior arising from two autocatalytic species. It was found that for an initial pH range of $3.5 < pH < 7.5$ the propagation velocity of the front is almost entirely insensitive to $[H^+]$. However, as pH is increased above 8.0, the front velocity depended highly on initial pH - it slowed as the pH was increased. This trend continued up to pH = 9.6, where above this value front propagation was not supported. For highly acidic initial conditions of pH < 3.0, velocities increased sharply as pH was decreased; at pH < 1.9 the reactant solution became too unstable to support front velocity measurements, as it was almost immediately converted to product. For the entire range of initial pH values, the pH of the product solution was always in the range $2.0 < pH < 3.0$.

More recent work on IAA fronts [9, 10] in horizontal layers has focused primarily on how electric fields affect the reaction. These studies have shown that a change in the

overall outcome of the reaction can arise when an electric field is applied. Reaction mixtures with various values of R were used to investigate the electric field effects on the net reaction stoichiometry. These experiments were performed in agar gel in order to prevent hydrodynamical flows in the reaction layer. The effect of starch concentration on front velocity in the IAA system was also investigated in [10]. In previous experiments [1,4,5], it was assumed that the starch indicator played a passive role in the IAA system, influencing neither the reaction mechanism nor the front propagation velocity. Both an experiment and a model [9,10] show conclusively that this is not the case; as starch concentration was increased it slowed down the front velocity.

1.3.2 IAA Fronts in a Thin Vertical Layer

The product of the IAA reaction is less dense than the reactant. Therefore when the reaction front propagates from below the buoyancy force created by the density difference between the reactant and the product left behind adds mass transport to the already complex reaction-diffusion problem. The coupling between reaction-diffusion and buoyancy driven convection can be studied in a quasi two-dimensional configuration by placing reactant in a vertically oriented slot and initiating the reaction along the entire length of the slot [11, 12]. Results from these investigations have shown that the buoyancy-driven instability causes an initially flat front to break up into fingers. The fingers arise from the competition between convection, which acts to extend the fingers, and diffusion, which acts to smooth the front. The spacing of the fingers has been found to depend on the width of the vertical slot.

For the vertical slot geometry, theory has been well developed and agrees well with experimental observations [13-16]. Linear stability analysis of a 2D flow model has shown the instability of a flat front. The theory predicts that the initial instability takes the form of a chain of convection rolls that turn the front into a series of rising fingers. The theory also shows that only low wave number perturbations will grow, damping out the higher wave numbers. The relative strength of the buoyancy force may be described by a dimensionless parameter that comes from linear analysis [17-19]

$$S = \frac{\delta g a^3}{\nu D_C},$$
(3.6)

where g is the acceleration due to gravity, a is the cell thickness, v is the kinematic viscosity, D_C is the diffusion constant of the autocatalyst, and $\delta = (\rho_u / \rho_r) -1$ is the dimensionless density jump between the reacted and unreacted solutions. For the IAA reaction, the density jump is almost completely due to the change in the partial molal values caused by the reaction, so the thermal expansion of the fluid due to the exothermicity of the reaction can be neglected [20].

1.3.3 IAA Fronts in Capillary Tubes

The motion of IAA fronts in vertically oriented capillary tubes can also be affected by convection induced by the density gradient across the reaction front. For descending fronts, no convection occurs since the fluid is bottom-heavy across the front. Ascending fronts, however, are top heavy across the front and free convection can result, provided that a critical value of the dimensionless parameter (Eq. 3.6) – where a represents the tube radius rather than the slot width - is exceeded. Convection is driven in the IAA reaction by the small amount of heat the reaction releases and by the positive volume of reaction that takes place. If instead the reaction induced a negative volume change that competed with the thermal expansion, the mode of convection that would occur is called double-diffusive or multicomponent convection.

The shape of the convecting front in the IAA reaction can take one of two possible forms: antisymmetric and axisymmetric (Fig. 1).
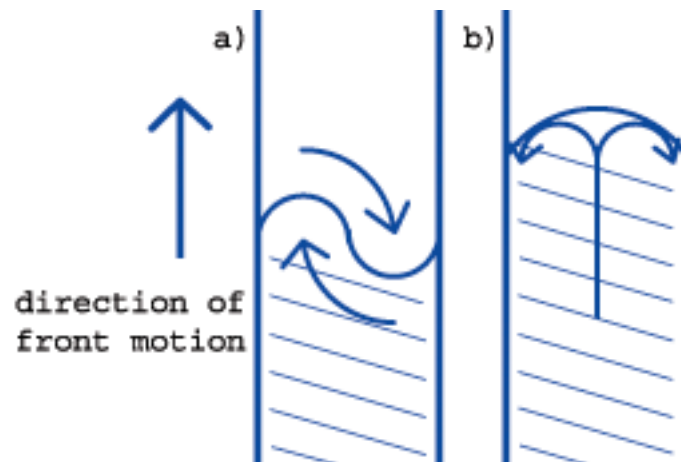

Figure 1.1: (a) Antisymmetric convection, (b) Axisymmetric convection.

Linear calculations [21] using the dimensionless driving parameter S predict that planar ascending fronts are unstable to nonaxisymmetric convection for $S \geq 87.9$ and to axisymmetric convection for $S > S_C = 370.2$. Nonaxisymmetric convection is therefore predicted to appear at the onset of convection. These critical S values have been verified experimentally [5, 22].

IAA front velocity in vertically oriented capillary tubes is affected by changing the driving parameter S. This is achieved most easily by performing experiments using capillary tubes with various radii while using solutions with identical chemical compositions. For S values below the critical value of 87.9 no convection occurs and front speeds are the same for both ascending and descending fronts [5]. Moreover, descending fronts have been found to have front velocities that do not depend on the internal radius of the capillary tubes [5, 22]. For ascending fronts, increasing tube radii acts to enhance convection and therefore increase the front speed.

Chemical composition also affects front velocity. Ascending and descending front velocities increase linearly as a function of increasing initial iodate concentration in excess arsenous acid solutions [1]. In excess iodate solutions the descending front velocities remain linear as a function of initial iodate concentration, however ascending velocities increase but not with a directly proportional relationship to initial iodate concentration [22]. The velocity dependence on initial arsenous acid concentrations is linear for both ascending and descending fronts in either the excess iodate regime or the excess arsenous acid regime. In the excess iodate regime, the slope of the lines for both ascending and descending fronts is much greater than that in the excess arsenous acid regime.

Convection always occurs in capillary tubes oriented horizontally [1]. Such a system is analogous to a system with fluid between two vertical, differentially heated plates, and is therefore unstable regardless of the tube radius. As a result, a horizontally propagating front is always faster than a pure reaction-diffusion front. Front velocity and shape in inclined tubes is not well understood, however it has been found that maximum front speed occurs for neither ascending fronts in vertical tubes nor fronts in horizontal tubes [23]. For a given capillary tube radius, there is an angle at which front speed will be at maximum. This affect has also been studied in similar chemical system; the

autocatalytic chlorite-thiosulfate reaction [24]. It was found that maximum front speed occurred between 40 and 60 degrees from the horizontal. This system is not, however, directly analogous to the IAA system since the reaction is highly exothermic, therefore causing the heat produced during the reaction to play a significant role in convection.

IAA fronts in horizontal capillary tubes have also been studied in the presence of electric fields [25] that act to affect the transport of ionic components. It has been shown that front velocity can be increased up to 10 times the normal velocity in a field with a negative gradient with respect to the front motion. Wave velocity can also be decreased in the positive field up to the point where propagation can be halted (where it may again propagate should the field be changed). Increasing the positive field up to a critical value can even completely annihilate the wave, regardless of if the field is removed after this point or not.

The most recent work on the IAA reaction in capillary tubes has been the theoretical and experimental treatment of front propagation coupled with externally introduced fluid flow [26, 27]. Through both theory and experiment it has been shown that an IAA front moving through a tube filled with fluid moving in the opposite direction will travel at the usual speed that it would have if no flow were present. In this situation the front develops a cusp at the center of the tube. Remarkably, the midgap cusp consumes just enough extra reactant to compensate for the flow, thereby allowing the wave front to travel at its usual speed.

1.4 Motivation

A considerable amount of work has been done on the propagation of the IAA front in various geometries. In narrow tubes the study of the front is essentially reduced to a one-dimensional problem. In the limit of thin vertical slots and horizontal layers the front behavior is two-dimensional. Naturally, this leads one to inquire about how the IAA front behaves in three dimensions. More specifically, the question that motivated the research detailed in this report was: How will the IAA front evolve in an essentially unbounded volume of still fluid if the reaction is initiated at a small point? One would expect that if there was no density gradient across the front and less importantly if the reaction was not slightly exothermic, that in fluid where no flow was present the front

would propagate outwards as a sphere, analogous to the circular front shape in thin horizontal layers. However, due to the density gradient, convection does enter the problem. The initial goal of this research was to simply determine through experiment how the morphology of the front evolves in a three-dimensional scenario.

Experiments revealed that the initiation of the front at a 'point' (a pipette tip) cannot be achieved, a finding that hindered the progress of the study of the IAA reaction in three-dimensions considerably. Rather than triggering a front that would propagate throughout an entire volume of reactant, the thin front that would rise out of the pipette tip would collapse and disappear. Thus, the reactant solution was left in its initial state. Much effort was placed into varying chemical composition of the reactant mixture in attempt to find a working solution that would allow the thin front to propagate throughout an entire reactant volume. This investigation turned out to be fruitless.

Abandoning the efforts to initiate the reaction at a point, reactions were initiated in a tube that had a much larger radius. Fronts rising out of the larger tube did propagate throughout an entire volume of reactant. The behavior of these fronts as they propagated upwards in a large tube with a supercritical S value of the order 10^7 is discussed in this report. These fronts were studied at different fluid temperatures and distinguishing characteristics of front motion in two different temperature ranges was observed. Experiments were also performed to determine how the IAA front velocity in capillary tubes changes as a function of temperature.

Chapter 2

Experimental Method

2.1 Chemical Preparation

Iodate solution was prepared from reagent grade KIO_3 powder. This powder dissolves easily in water at room temperature. Stock solution was prepared by dissolving an appropriate amount of powder first in 100 mL of distilled water and then further diluting that solution by adding 900 mL more distilled water. The concentration of the prepared stock solution was 0.1 M.

Arsenous acid was prepared from reagent grade As_2O_3 powder. 20.00 ± 0.01 g of As_2O_3 powder was initially dissolved in 500 mL of distilled water by stirring and heating (not to a boil) the powder for several hours in a sealed 2L flask. Following this 500 mL more distilled water was added to dilute the solution. The solution was heated and stirred until all the powder was dissolved. The exact concentration of arsenous acid produced by this procedure was not determined. To determine arsenous acid concentration one must use a procedure usually used to standardize iodine solutions [28].

Working solutions were prepared by diluting an appropriate amount of each of the desired stock solutions separately, and then mixing them together. Determination of the concentration regime (excess iodate or excess arsenous acid) of the working solution was done qualitatively by observing the colouration of the wake of the chemical front when using starch indicator. For a thin layer of solution in a Petri dish, excess arsenous acid solutions produced a thin blue front in an otherwise clear solution, while excess iodate

solutions left blue colouration in the wake of the front. In all instances when starch indicator was used it composed .04% by weight of the solution.

The other indicator that was used to visualize the reaction front was congo red. The use of congo red was made possible by not using buffer solution to control the pH of solution. Solutions containing congo red indicator appear red when the pH is above ~5.2 and they appear blue for pH values below this value. Since the reaction front produces hydrogen ions autocatalytically, it produces product solution that has a pH well below 5.2, and thus it appears blue. Congo red solution was prepared from congo red powder by dissolving 0.1g in 100 mL of distilled water. For every 100 mL of working solution produced, 3 mL of congo red solution was added in order to clearly visualize the front.

2.2 Reaction Initiation

The IAA reaction can be initiated at the negatively biased part of a platinum electrode. This method was, however, seldom used for the experiments discussed in this report. When applying a voltage across an electrode in IAA solution it does indeed trigger a reaction front, however it also introduces heat and bubbles into the solution. For experiments that require the reactant solution to remain still, the introduction of heat and bubbles into the solution cannot be tolerated. Therefore, another means was used to initiate the reaction front; the injection of a small amount of concentrated hydrochloric acid. The method by which the acid was injected into solution is discussed in section 2.3.

2.3 Initial Test Apparatus

The purpose of the test apparatus was to get an initial idea on IAA front behavior in three dimensions before constructing a temperature controlled apparatus to house the experiment. The test apparatus consisted of either a 250 mL or 500 mL Erlenmeyer flask with an appropriate size rubber stopper, a standard size pipette (a length of 14.2 cm, a tip diameter of 0.9 mm, and a base diameter of 5.5 mm), and a clamp held in place with a cement block. The pipette was inserted through a hole drilled through the stopper. The seal between the pipette and the hole was watertight. With the pipette tip pointing inside

the flask, the modified cap was used to seal reactant solution placed inside. A length of clear tubing 3-4 cm in length was placed on the outside end of the pipette with a cotton plug placed inside the tubing. The open end was closed with a large clip completely sealing the reactant inside the apparatus, allowing it to be turned upside down and placed in a clamp. By squeezing the tubing at the end of the pipette the air inside it and the pipette was pushed into the solution thereby filling the pipette with reactant. Many of these apparatus were constructed and used simultaneously. Once they were set up they were left alone typically 8 hours or longer before the reaction was triggered. The reason for the long wait was to allow for the fluid motion to completely die away.

Reactions were triggered by injecting a small amount of hydrochloric acid below the cotton plug. The presence of the cotton plug was to prevent the introduction of any type of fluid flow from the injection process. To inject the acid, a syringe with a thin needle was used to penetrate through the rubber tubing. Injections made at an approximately 30 degree angle to the tubing would allow for the hole created by the needle to seal on its own once the needle was removed. As a precautionary measure a small strip of electric tape was placed over the hole. Once initiated, the reaction would slowly move through the cotton plug and up the pipette towards the solution contained in the flask.

2.4 Capillary Tube Apparatus

All capillary tube experiments were performed in a fluid jacket. The fluid jacket was 65 cm long, with an inner diameter of 3.4 cm with a wall 2 mm thick. The jacketed capillary tube apparatus was constructed by drilling two holes in each of two rubber stoppers: one hole in the center to place over the end of the capillary tube and the other hole through which a small copper pipe was fitted. To each copper tube a rubber hose was attached which was used to connect the apparatus to a Neslab RTE-111 fluid bath capable of controlling the temperature of the fluid in the jacket to the nearest tenth of a degree. The apparatus was connected by means of three clamps to a sturdy frame attached to an optical table that held it in a vertical position.

Three different capillary tubes were used for this experiment, with diameters of 1.32 mm, 2.56 mm, and 3.03 mm. The diameters of the tubes were determined by finding the difference between the weight of the tubes with water in them and without. The diameter could then be calculated using the density of water at room temperature. The reaction fronts were initiated at the bottom of the capillary tubes by the usual method - injection of a small amount of acid into a clear tube just below a cotton plug. Between each run the capillary tubes were flushed with distilled water and then with reactant before they were refilled. Front speeds were determined by tracking the position of the front as it moved through the tube. This was done by means of viewing the front through a cathetometer that moves vertically on an attached Vernier scale. The position of the front at specific times was recorded to the nearest second over intervals of 5-10 minutes for at least an hour. For each capillary tube front motion was tracked at five different temperatures: 5.0, 12.5, 20.0, 27.5, and $35.0 \pm 0.1°C$. The fronts were made visible by means of congo red indicator. The chemical composition of the reaction mixture was kept constant for all runs at $[KIO_3] = 0.005$ M and 10% arsenous acid stock solution.

2.5 Supercritical Tube Apparatus

A picture of the supercritical tube apparatus is shown in Fig. 2.1. The construction of the apparatus was similar to the construction of the capillary tube apparatus. The supercritical tube (length 110 cm, diameter 2.8 cm, wall width 0.2 cm) was placed inside a larger tube (length 89 cm, diameter 8.9 cm, wall width 0.2 cm) and held in place by means of a large rubber stopper. Two holes were needed in each stopper: one at the center for the tube and the second through which a copper tube was placed. The copper tubes were attached to hoses connecting the apparatus to a Neslab RTE-111 water bath. The control of the bath used for this experiment was able to control the temperature of the circulating water to the nearest hundredth of a degree.
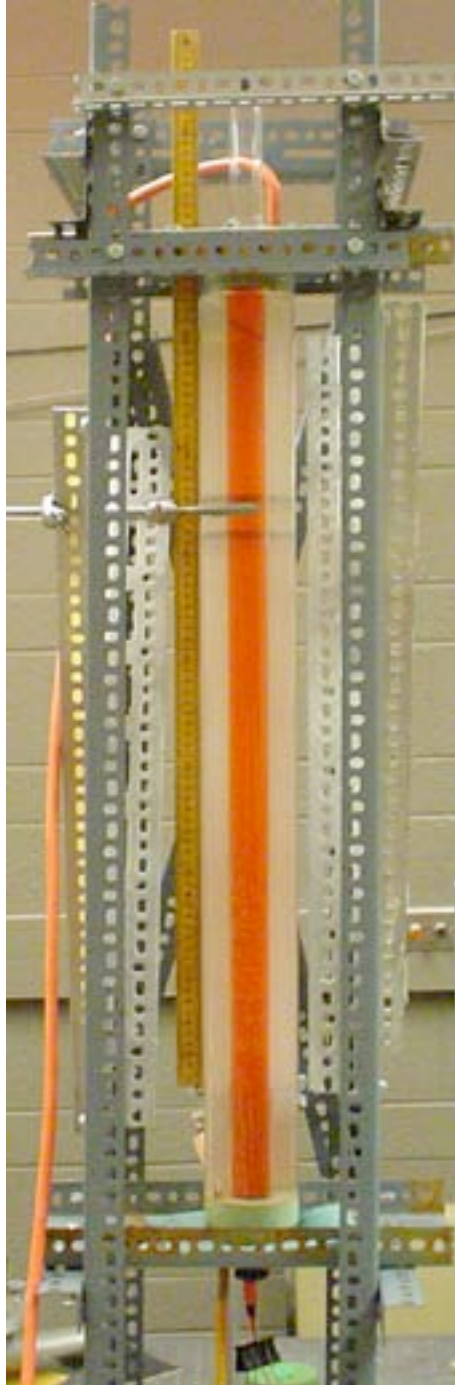
Figure 2.1: A picture of the supercritical tube apparatus.

The glass tubes were held upright by means of tower constructed from Dexion that was mounted on an optical table. The bottom part of the tubes were placed on top of rubber padding attached to a platform on the tower with a hole large enough to fit the protruding end of the inner glass tube and the copper tube through. The upper part of the glass tubes apparatus was held in place by another identical platform with the rubber padding facing downwards. There were also two large clamps attached to the tower holding the tubes in place. Careful attention was paid to the sturdiness of this set-up to ensure that the tubes would be kept still at all times

A rubber stopper was fitted to the bottom end of the protruding inner tube. Through a hole in this rubber stopper a glass tube with clear tubing attached at its open end was inserted, a clip was then used to seal the tubing. As usual, a cotton plug was placed inside the tubing to prevent flow when acid was injected to initiate the reaction front. Reactant was placed inside the inner tube by pouring it through the open end at the top. The reactant composition for this experiment was equivalent to that used for the capillary tube experiment. Between each run of the experiment the inner tube was soaked with distilled water and then wiped down by pushing a ball of paper towel through it with a long rod. The tube was then flushed with a small amount of reactant before refilling it for another run. Once filled, there was a period of at least twelve hours before the reaction was initiated to allow for all residual fluid motion to subside.

The motion of the front was recorded by means of digital images. A meter stick was placed next to the tube so that the height of the front could easily be determined from each picture. The time each picture was taken was recorded to the nearest second. Typically, the time between successive pictures was between 5 and 10 seconds. Experimental runs were carried out at four different temperatures, 12.50, 20.00, 27.50 and 35.00 ± 0.02 °C. It was not possible to do experiments at 5 °C as the temperature bath could not keep the large volume of fluid at that low a temperature unless the tubes were insulated, which would have interfered with visualizing the front.

Chapter 3

Observations and Results

3.1 Front Collapse

The test apparatus discussed in section 2.3 was used to study front collapse. It was initially assumed that once the reaction was triggered and a front developed, that it would then make its way out of the pipette and eventually propagate throughout the entire reactant solution. This was, however, not what was observed. Typically a small sphere of product would form at the pipette tip. The sphere would then rise upward and result in a thin filament of product solution extending from the pipette tip into the reactant solution. The filament would then slowly fade away until it was no longer visible. Product solution remaining inside the pipette would cause this process to be repeated, sometimes before a previously formed filament had time to completely disappear. Over the course of hours, the emergence of new filaments would discontinue leaving the system in a state where product would be inside the pipette up to typically 5 mm from the tip, and the rest of the solution in the apparatus would remain reactant. Left alone for days, this situation would not change. The exception being for instances when the reaction triggered spontaneously at the surface of the reactant solution inside the flask. In this situation reactant would eventually be completely consumed by product.

When front collapse was initially observed, it was assumed that somehow the solutions being tested were not excitable enough for front filaments to propagate through the reactant. In light of this, runs in the test apparatus involving variations of chemical

concentration of the reactant solution were implemented. For these experiments, the concentration of IO_3^- was held constant at 0.005 M (a standard concentration used for the study of the IAA reaction [1, 5]) while either pH or arsenous acid concentration were varied. When testing for solutions with $[IO_3^-] < 0.0025$ M reaction fronts were difficult to initiate, and therefore these low concentration solutions were abandoned early in the testing process.

The influence of acidity on front death was studied by varying the pH of reactant solution between 2.49 and 7.16. For pH values greater than 5.2 tests were performed on solutions containing either congo red indicator or starch, or sometimes both. Below a pH of 5.2 only starch indicator could be used, since congo red is always blue in this range regardless of whether or not a reaction front is present. Performing tests for solutions below a pH of approximately 4.6 was nearly impossible. Usually within minutes, but almost certainly before 8 hours after placing the reactant solution in the test apparatus, a reaction front would spontaneously trigger at the fluid surface – not allowing for tests to be performed. In the few instances when this did not occur filaments of rising product would fade as usual. Filaments that managed to reach the top of the fluid before they faded away, however, sometimes seemed to be able to initiate a reaction front at the fluid surface that would then proceed to engulf the entire reactant solution. In experiments performed in which the flask was filled to capacity leaving no liquid-air interface this did not occur. For solutions with a pH above approximately 4.6, spontaneous reaction at the surface rarely occurred within the initial 8-hour period after mixing for. However, left for days these solutions would spontaneously trigger. The longer lifetime of these solutions allowed for more extensive testing of the filament behavior in this pH region. Nonetheless, results didn't show any sort of different behavior for any of the solutions. The product managed to make its way out of the pipette tip only to form a filamentous front that always collapsed leaving the reactant solution in its initial state.

In addition to the pH tests, varying the amount of stock As_2O_3 solution did not change the collapsing of thin reaction fronts. Solutions containing from 1.25 - 50% of the stock arsenous acid solution were used, varying the pH for solutions with equivalent amounts of arsenous acid. Above 5% stock arsenous acid solution, reactions using iodine

indicator in petri dishes displayed a thin blue propagating front in an otherwise clear solution, clearly indicating that the solution was in the excess arsenous acid regime.

The collapse of thin rising reaction front filaments was unexpected. To our knowledge this phenomena has not been reported for any system that supports chemical reaction fronts. The only similar type of phenomena akin to front death that has been reported is for a system supporting chemical reaction pulses. Toth et al. [29] reported that for thin layers of excitable BZ mixtures connected by capillary tubes there is a critical tube diameter below which an exiting pulse will collapse and cause wave propagation to cease. Hence, for a thin BZ layer, a critical nucleation size is necessary to initiate a wave.

At this point, it seems as if we have stumbled upon behaviour similar to BZ critical nucleation size in the IAA reaction. The study of this phenomenon for the IAA reaction in three dimensions, however, is complicated by mass transport that causes any sort of small pocket of product solution to rise and be smeared out into a thin filamentous shape. It therefore seems that below a critical size mass transport acts to hinder front propagation, rather than enhance it.

3.2 Capillary Tube Experiment

The relationship between temperature change and front speed in vertical capillary tubes was determined. Front speed was calculated by tracking the position of the front as a function of time using a cathetometer. The front rise was linear with time for all capillary tubes at all temperatures maintained during experiments, allowing for velocities to be determined simply by calculating the slope of the line. The velocities are shown as a function of temperature in Fig 3.1. The slopes of each of these lines were calculated and are shown in Table 3.1.

The shape of the fronts in the 2.56 mm and 3.03 mm diameter tubes were axisymmetric, clearly indicating that convection was taking place. The fronts were flat for the 1.32 mm diameter tube experiments, indicating that convection was not occurring, leaving reaction-diffusion as the only means of propagation for the front. In the 1.32 mm tube front speed was also determined for the downward direction. According to both theory and experiments [4, 5] that used starch as an indicator in buffered solutions,
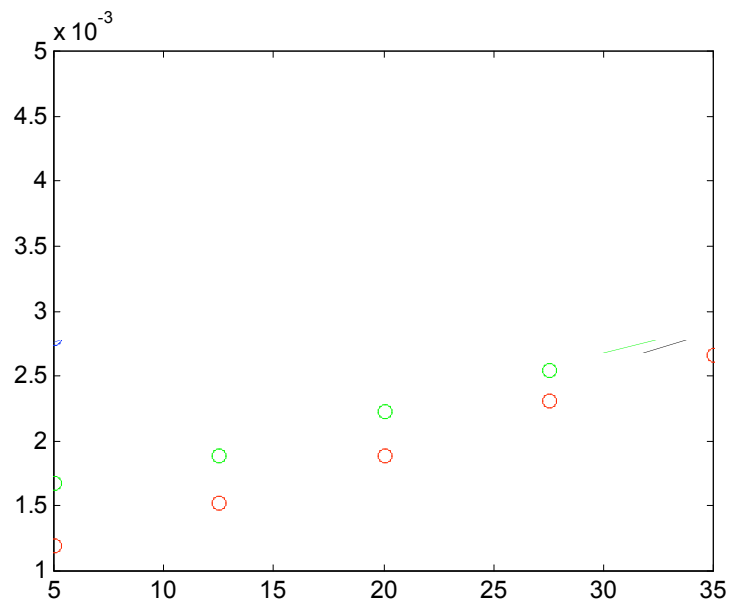
Figure 3.1: Upwards front velocity as a function of temperature including linear fits for the front in three capillary tubes. Tube diameters are 1.32 mm, 2.56 mm, and 3.03 mm. The downward front velocity for the 1.32 mm capillary tube is also included.

Tube Diameter (mm)	Front Direction	Slope $\times$ 10^{-5} (cm/s°C)
1.32	down	5.2 ± 0.2
1.32	up	5.0 ± 0.1
2.56	up	4.2 ± 0.2
3.03	up	6.2 ± 0.1

Table 3.1: Calculated slope values for the change in front speed as a function of temperature.

front speed should be equivalent in both the upward and downward directions for tubes in which convection does not occur. Surprisingly, for all 5 temperatures at which experiments were performed, the downward front velocity was slightly greater than the upward velocity for the 1.32 mm diameter tube. However, the linear relationship between front velocity and temperature for both upward and downward front motion are equivalent within error.

Opposite trends in the linear relationship between temperature and front velocity are seen for the two tubes in which convection does occur. The 2.56 mm diameter tube front has a slope less than that for the pure reaction-diffusion front. As a result, the velocity of the 2.56 mm front moves closer to the non-convecting front speed as temperature is increased. The 3.03 mm diameter tube, however, has a slope greater than the slope for the 1.32 mm tube, indicating that temperature has a stronger influence on front propagation for this tube than it does on the others. However, since the two tubes that support convective front motion showed different trends in their linear relationships, it is not clear what the difference is (if there is one) between how temperature affects front motion in tubes that support convection and tubes that do not.

3.3 Supercritical Tube Experiment

The supercritical tube experiment was carried out at 4 different temperatures: 12.50, 20.00, 27.50, and 35.00 ± 0.02 °C. The behaviour of the rising fronts in the experiments performed at 12.50 °C and 20.00°C was markedly different from the behaviour of experiments with the temperature held at 27.50 °C and 35.00 °C. In the first two subsections, distinguishing features of plume behaviour for each temperature are described, while analysis of the rise time and plume width are discussed in the final two subsections. For the sake of convenience, the temperatures 12.50 °C and 20.00 °C are classified as the low-temperature domain, while the high-temperature domain refers to the temperatures 27.50 °C and 35.00 °C.

3.3.1 Writing and Snowballing Plumes

In the low-temperature domain the chemical front forms a plume that writhes its way up the tube. As it does so, the plume increases in size and the product left in its wake converts the reactant in its vicinity to product. Once the twisting plume reaches a certain height, the motion becomes almost entirely vertical as the writhing motion dies away. The writhing motion and the transition to relatively straight vertical motion is shown in Fig. 3.2. The height at which the twisting stopped was different for the 12.50 °C and 20.00 °C runs: for three experimental runs held at 12.50 °C twisting stopped at an average height of 36.9 cm above the point where the front entered the supercritical vessel, for the three runs at 20.00 °C the average height where the plume began to rise straight up the tube was 30.9 cm.

A similar type of zigzag motion in a fluid experiment is observed in the path of air bubbles rising in water, for both two-dimensional [30] and three-dimensional [31] systems. In both systems, straight bubble motion gives way to zigzag motion once the Reynolds number exceeds a critical value. The zigzag motion is driven by vortex shedding in the wake of the bubble. Strangely, the plumes in the IAA reaction exhibit zigzag motion in the low-temperature domain, where the Reynolds number is lower than in the high-temperature domain where plumes rise in a straight path.

Another feature of front behavior at 12.50 °C and 20.00 °C is the formation large plumes below the leading smaller plume. As the plume from below rises it collects product left in the wake of the leading front (i.e. the front with the highest vertical position) and consequently the snowballing of the lower plume causes it to accelerate upwards. Eventually the snowballing plume reaches the lead plume and engulfs it, as shown in Fig. 3.3.

As plume fronts rise they generally increases in size, however, in the low-temperature domain there were instances where a small front filament broke away from the bulk and took over as the leading front. Like what was observed for the front filaments rising out of the pipette tip, these breakaway front filaments also collapsed and disappeared. Thin front collapse in the supercritical experiment is shown in Fig. 3.4. Typically this phenomenon occurred in the early stages after the front made its entrance from the smaller tube into the supercritical tube.

Figure 3.2: Four pictures for an experimental run at 12.50 °C detailing the transition between writhing to relatively straight vertical plume motion. The same 30 cm length of the tube is shown in each picture. At ~556s writhing motion has given way to straight rising.

Figure 3.3: Three pictures for an experimental run at 20.00 °C detailing the snowballing of the lower part of a plume that eventually engulfs the plume head. The same 30 cm length of the tube is shown in each picture.

Figure 3.4: Three pictures for an experimental run at 12.50 °C detailing the collapse of a front filament. The same 28 cm length of the tube is shown in each picture.

3.3.2 Straight Rising Plumes

The rising plume fronts in the experiments performed in the high-temperature domain rose in a straight path, a striking contrast to the writhing plume motion observed in the low-temperature domain. A straight rising plume is shown in Fig. 3.5. Similar to the plumes in the low temperatures domain, plumes generally grow in size as they make their way up the tube.

Another difference between the high and low temperature domain plumes was the absence of the snowballing effect in the high-temperature domain. In every run done at 12.50 °C and 20.00 °C, a juggernaut plume rising from below eventually overtook the leading plume. In the high-temperature domain this did not happen, the leading front remained so for the entire length of the tube. In addition, reactant filaments were not observed in the high-temperature domain experiments. Thus, front collapse was also not observed.

3.3.3 Rise Time

From digital pictures taken to record the reaction front evolution, the position of the leading front was determined and was plotted for each temperature as a function of time in Figs. 3.6 - 3.9. These figures show results from three experimental runs at each of the four temperatures for which experiments were held. Where possible (where the data is linear) slopes were calculated, thus determining plume velocity. As one would expect based on the observed differences in behavior between fronts in the high and low temperature domains, very different trends in the data are also observed. Two of the three runs (runs 1 and 2) at 12.50 °C shown in Fig. 3.6 show similar trends. For each of these data sets the plumes twisted their way up to a point where a snowballing plume from below caught the leading plume and the motion of the front became almost exclusively vertical. The respective points where this occurred coincide with where the two plots become linear. Velocities calculated from the slopes of these linear portions of data give rise velocities of 0.109 ± .001 cm/s for run 1 and 0.091 ± .001 cm/s for run 2. For run 2, the linear portion of the plot does not continue to the end of the tube like for run 1. The
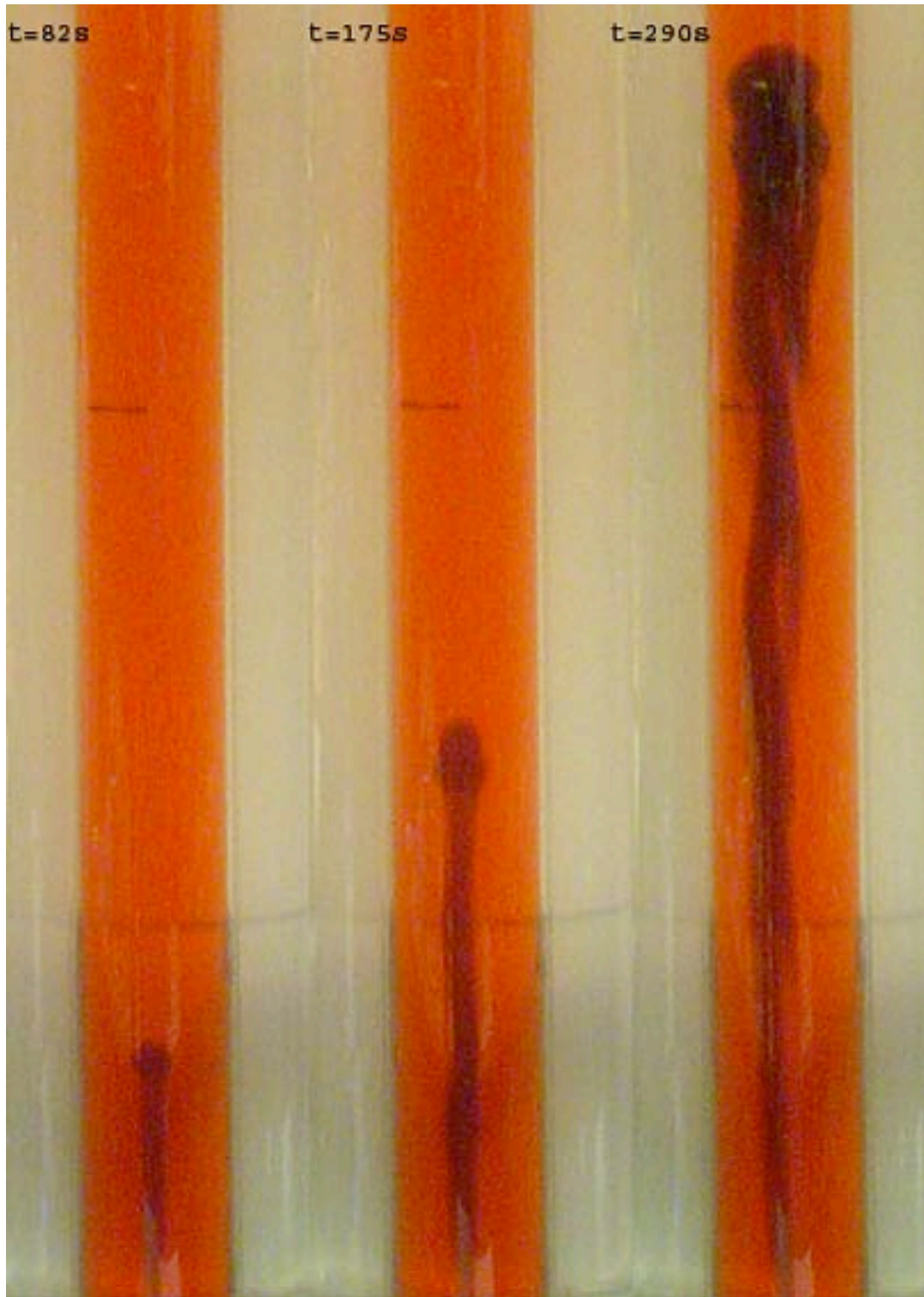
Figure 3.5: Three pictures for an experimental run at 27.50 °C showing the straight rise of a plume. The same 32 cm length of the tube is shown in each picture.
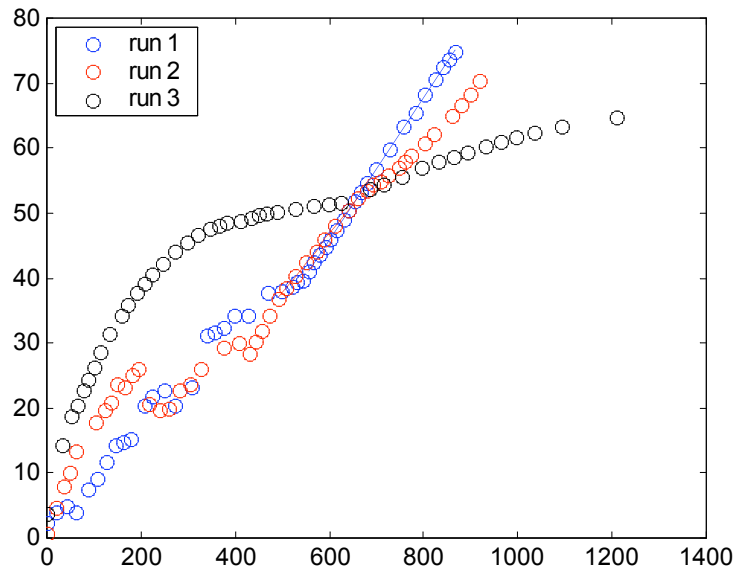
Figure 3.6: Vertical displacement as a function of time for three runs at 12.50 °C. Where applicable, lines of best fit are shown in the colours assigned to each data set.
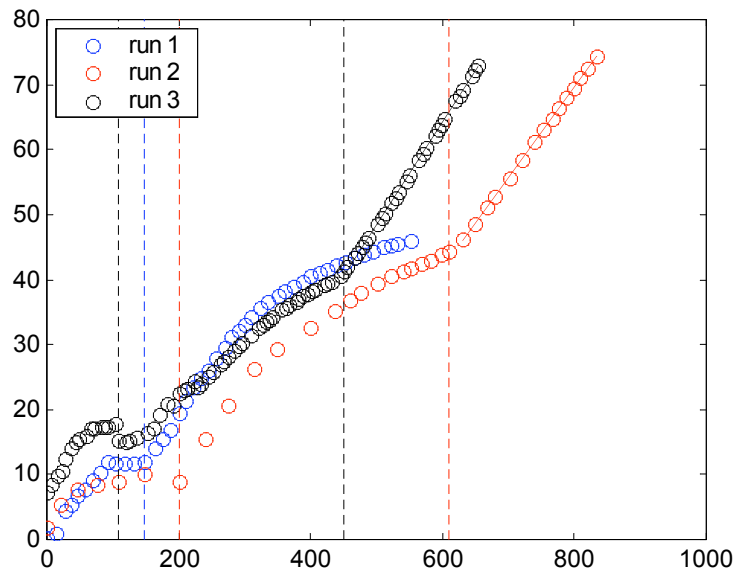

Figure 3.7: Vertical displacement as a function of time for three runs at 20.00 °C. Where applicable, lines of best fit are shown in the colors assigned to each data set. Also shown in the assigned colours are vertical dashed lines separate the three regions where different plume behavior is observed: region 1 is where the front decelerated, eventually stagnating for a short period of time; region 2 is where a plume head formed that writhed up the tube; and region 3 is where a snowballing plume caught up to and engulfed the lead plume.
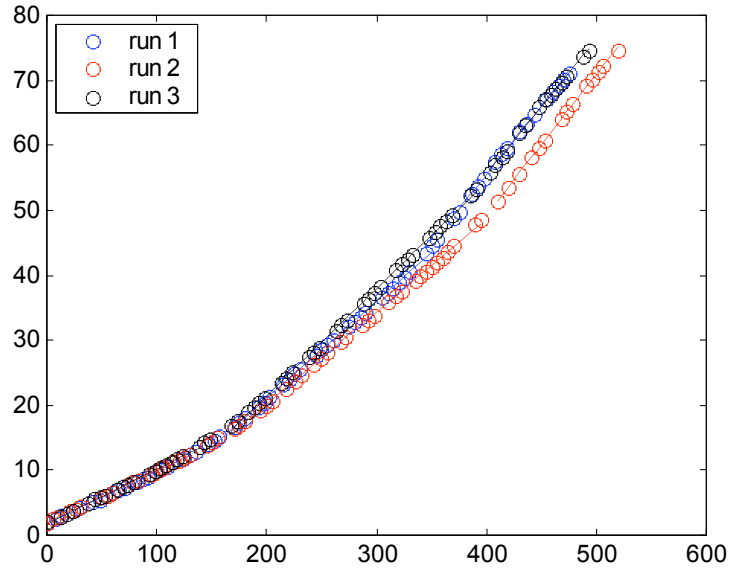
Figure 3.8: Vertical displacement as a function of time for three runs at 27.50 °C. Lines of best fit are shown in the colours assigned to each data set.
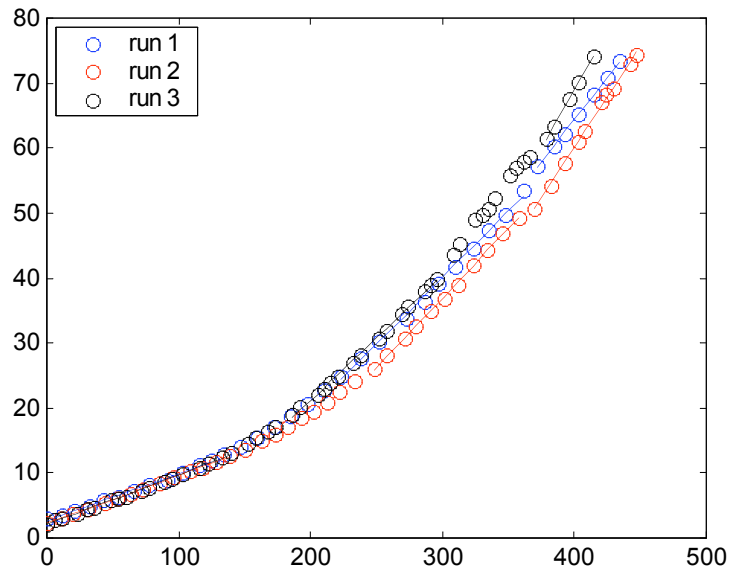

Figure 3.9: Vertical displacement as a function of time for three runs at 35.00 °C. Lines of best fit are shown in the colours assigned to each data set.
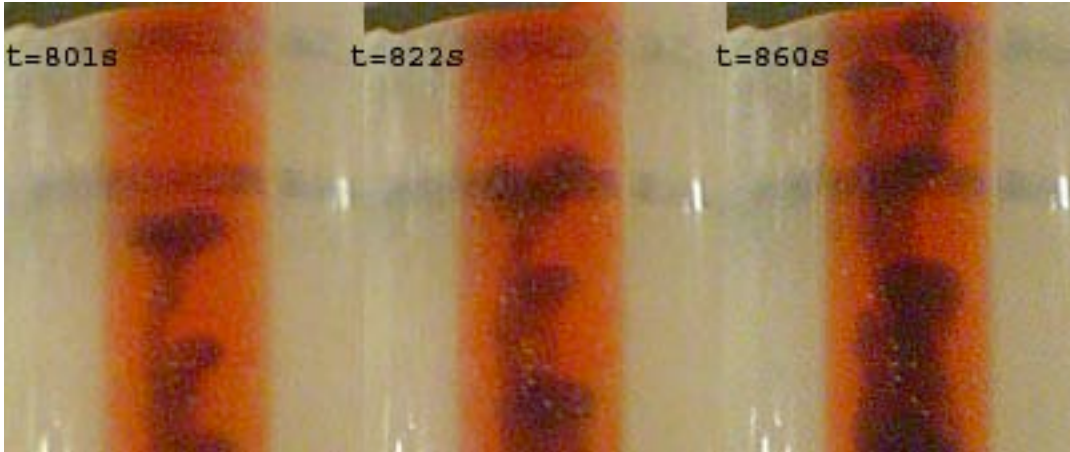
Figure 3.10: Three pictures for an experimental run at 12.50 °C showing plumes breaking up into multiple plumes. The same 8 cm length of the tube is shown in each picture.

linear motion was destroyed in this case by an occurrence unique to this run: the single plume broke apart and formed multiple plumes as shown in Fig. 3.10. The rise time data for run 3 looks completely different than the data for runs 1 and 2. For run 3 the plume initially rose much faster than in the other runs, it then decelerated rapidly. In addition, the plume width did not grow to be as large as in the other runs and snowballing did not occur at the point where plume lateral plume motion dissipated. The growth of plume width is discussed further in section 3.2.4.

The experiments carried out at 20.00 °C have trends in rise time data that are consistent, showing three distinct regions of front plume behavior. These three regions are separated by vertical dashed lines on Fig. 3.7. In region 1 the fronts twisted until they remained for a short amount of time at a stagnation point. Region 2 is where the fronts grew out of their stagnation points and formed a plume head that twisted until it reached another critical position where writhing motion discontinued and the lateral plume motion became obsolete. Unlike the 12.50 °C runs 1 and 2, the writhing motion for runs at 20.00 °C did not die away as a consequence of snowballing – snowballing did not occur until much later. However, similar to the 12.50 °C runs 1 and 2, plume rise time became linear at the point where a snowballing plume engulfed the leading plume (region 3). Run 1 for the 20.00 °C data does not have data in region 3 because of a loss of power to the digital camera shortly before the snowballing plume reached the lead plume.

Rise time data in the high temperature domain (Figs 3.8.and 3.9) are similarly split into three regions. In this case, however, all regions have linear data, leaving the slope value as the only distinguishing characteristic between each region. The plume velocities calculated for each region from the rise time data are discussed in the following section. Figs. 3.11 and 3.12 show the rise time data from Figs. 3.8. and 3.9 with the linear fit for region 1 subtracted from all data for the respective run in order to better visualize the transition between each region.
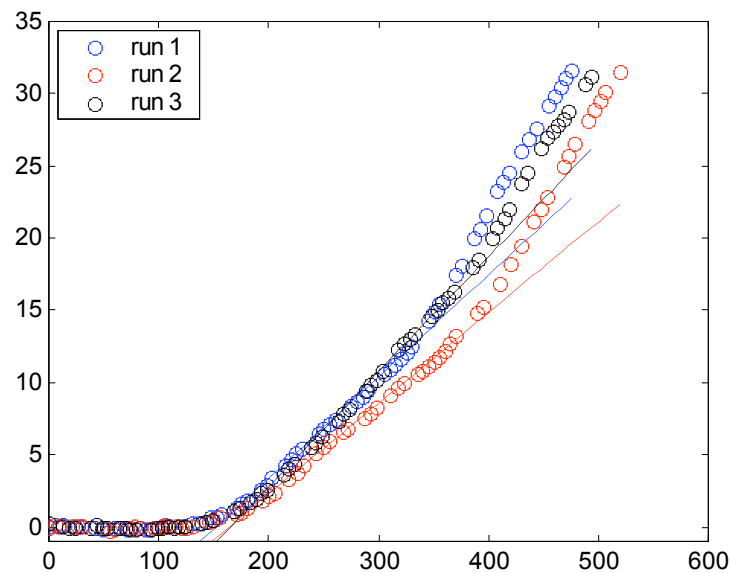

Figure 3.11: Adjusted vertical displacement as a function of time for runs at 27.50 °C. The linear fit to region 1 for each respective run was subtracted from the data. The linear fit for the region 2 data is shown as a line in the assigned color for each data set.
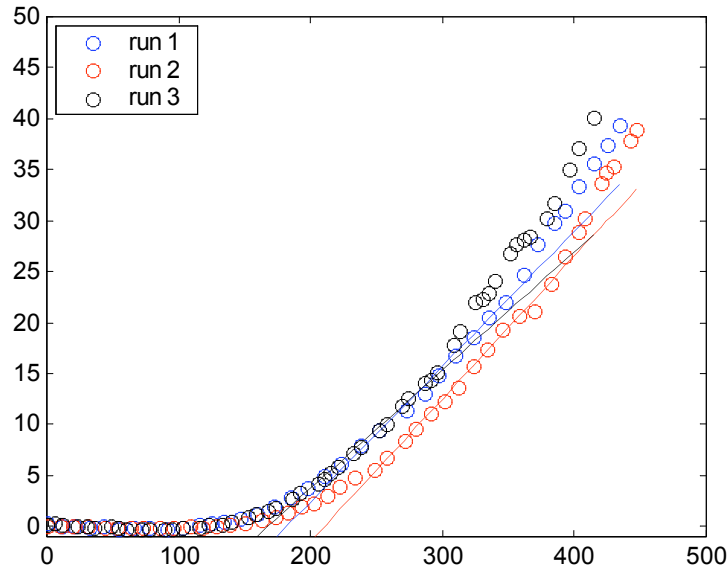
Figure 3.12: Adjusted vertical displacement as a function of time for runs at 35.00 °C. The linear fit to region 1 for each respective run was subtracted from the data. The linear fit for the region 2 data is shown as a line in the assigned color for each data set.

3.3.4 Plume Width and Velocity

In addition to the rise time data collected, the width of the plume head was also determined from the digital pictures of plume evolution. Plume width as a function of front height for the runs done at 12.50 °C are shown in Fig. 3.13. For runs 1 and 2 the plume width stays below 0.5 cm until the leading front is caught by a snowballing plume (recall this is also where the rise time data becomes linear for these runs). When the snowballing plume takes over as the leading front the width of the plume generally grows as it rises, up to 2.02 cm for run 1 and 1.80 cm for run 2. As mentioned previously, the front in run 3 showed different behavior than in the first 2 runs - the plume width did not grow to be as large as in the other runs. The maximum plume width achieved during run 3 was a mere 1.05 cm. The plume width data for the 20.00 °C run is shown in Fig. 3.14. For all three cases a general increase in plume width is shown past the points where a snowballing plume takes over as the front plume. Following approximately 5 cm after that is the region 3 data as identified in the rise time data. As the plot shows, the plumes

are already well into a period of growth before the rise time data becomes linear in region 3. The plume width data does not show any distinct change as the plume moves from rise time regions 1 and 2.

Figs 3.15 and 3.16 show the plume width as a function of height for the two temperatures in the high-temperature region. The three regions where rise velocities change are identified in these figures with dashed vertical lines. The average plume widths for each region are plotted against the regional rise velocity in Figs. 3.17 and 3.18. These figures show that the relationship between plume width and rise velocity is not directly proportional. From the average plume width and rise velocity data, the average Reynolds number for the flow in each velocity region at 27.50 °C and 35.00 °C is shown in Table 3.2, along with the average Reynolds number for the regions in the 12.50 °C and 20.00 °C where rise time data is linear. Here the Reynolds number Re is defined as Ud/ν, where U is the front plume velocity, d is the width of the front head, and ν is the kinematic viscosity of water. In the three-dimensional bubble experiment mentioned previously in section 3.1.1, an instability in the path of rising bubbles takes place at a critical Reynolds number of 275 ± 25. The Reynolds numbers for the rising plumes in this experiment are much less than this value.
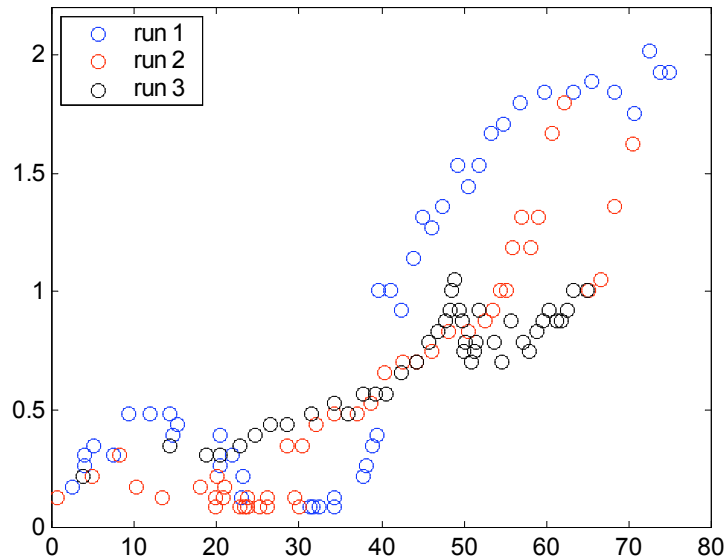

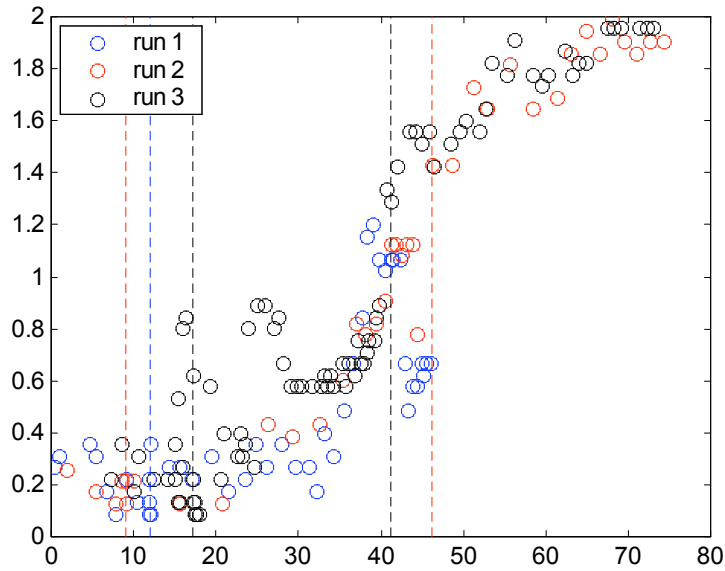**Figure 3.13:** Plume width as a function of height for three runs at 12.50 °C.

Figure 3.14: Plume width as a function of height for three runs at 20.00 °C. In the colors for each respective run, vertical dashed lines separate the three regions where different plume behavior is observed: region 1 is where the front decelerated eventually stagnating for a short period of time; region 2 is where a plume head formed that writhed up the tube; region 3 is where a snowballing plume caught up to and engulfed the lead plume.
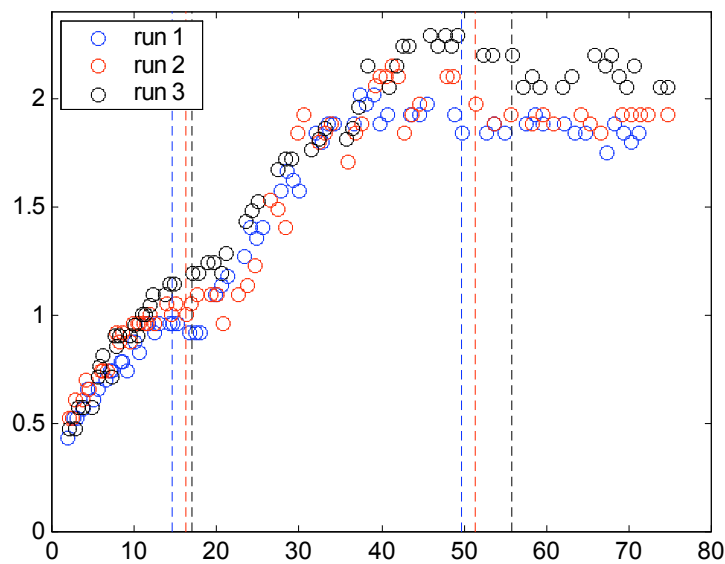

Figure 3.15: Plume width as a function of height for three runs at 27.50 °C. Vertical dashed are shown in the colors assigned to each run to show where the rise velocity changed in that particular run.
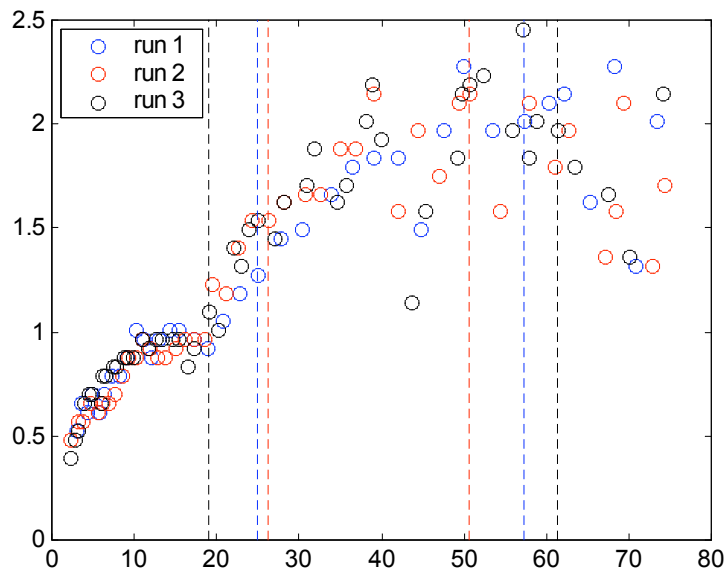
Figure 3.16: Plume width as a function of height for three runs at 35.00 °C. Vertical dashed are shown in the colors assigned to each run to show where the rise velocity changed in that particular run.
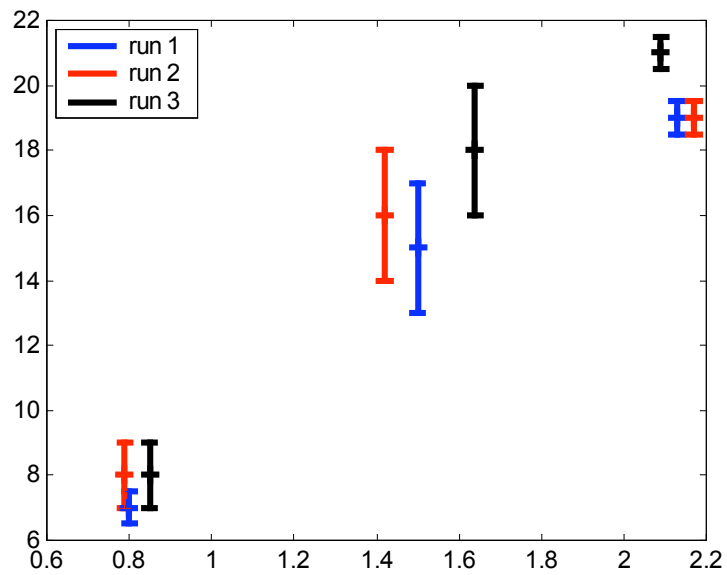

Figure 3.17: Average plume widths for each region plotted against regional rise velocity for three runs at 27.50 °C.
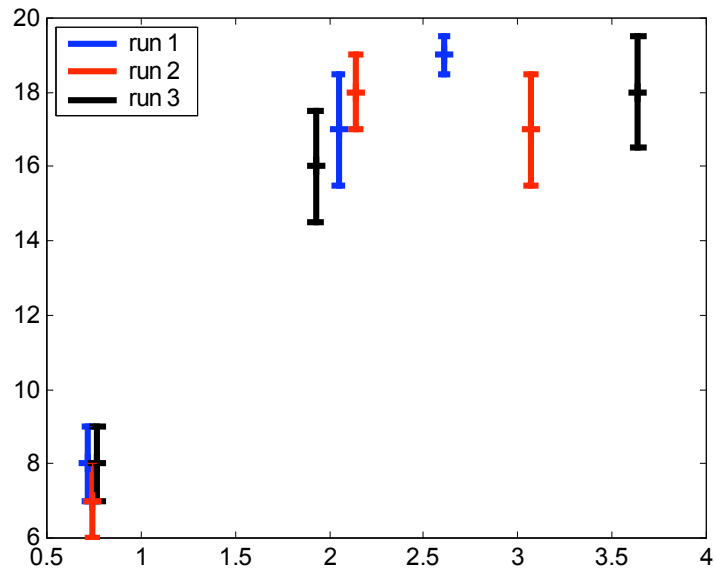
Figure 3.18: Average plume widths for each region plotted against regional rise velocity for three runs at 35.00 °C.

Temperature (°C)	Region	Mean Reynolds Number
12.5	linear rise time region	9.7
20.0	3	26.0
27.5	1	7.3
27.5	2	29.3
27.5	3	49.2
35.0	1	8.4
35.0	2	51.5
35.0	3	82.6

Table 3.2: The mean Reynolds number calculated for regions where plumes rose linearly with time.

Chapter 4

Conclusion

Groundwork for the study of the IAA reaction in three dimensions has now been established. Chemical front plumes that form in a supercritical tube have been found to have distinguishing characteristics in experiments performed at different temperatures. At temperatures of 12.50 °C and 20.00 °C, plumes have shown writhing motion that gives way to straight rising motion, whereas at temperatures of 27.50 °C and 35.00 °C plumes have shown no tendency towards twisting. In the upper two temperature experiments, the vertical displacement of plumes as a function of time has been found to have three distinct regions in which the velocity in each region is constant. For the lower temperature plumes, the relationship between vertical plume displacement and time has a much more complex relationship. In addition, other distinguishing features between the upper and lower temperature plume experiments are front collapse and snowballing, behaviours that have only been observed at the two lower temperatures.

There are many directions in which the study of chemical wave plumes can go from here. A physical explanation for the difference in plume behaviour at different temperatures must be established. Visualization of the flow profile of the fluid would aid in providing such an explanation. This could be achieved by means of tracer particles placed in solution that are matched to the density of the reactant. In order to help explain the IAA reaction plume behaviour, IAA plumes must be compared to the behaviour of non-reactive plumes and double-diffusive plumes. Simplifying the plume motion may

also help provide a better picture of the factors that affect plume motion. To simplify the motion, the Reynolds number could be lowered by adding an inert fluid such as glycerin (that would increase the viscosity of the fluid). Doing so may quench some of the more complex plume front activity, in turn decreasing the difficulty of the problem. Other simple additions to the experiment such as variation in chemical composition and performing experiments at temperatures other than those used in this work may also be useful for providing insight into plume behaviour. Using a large quasi two-dimensional vertical cell may also be a useful pursuit. Instead of initiating the reaction along the entire length of the cell as done in previous experiments using a thin vertical slab, the reaction could be initiated in a small region, thus creating a two-dimensional analogue of the supercritical tube experiment.

Bibliography

[1] A. Hanna, A. Saul and K. Showalter, *J. Am. Chem. Soc.* **104**, 3838 (1982).

[2] R.J. Field and R.M. Noyes, *J. Am. Chem. Soc.* **96**, 2001 (1974).

[3] P.A. Epik and N.S. Shub, *Akad. Nauk. SSSR* **100**, 503 (1955).

[4] T.A. Gribschaw, K. Showalter, D.L. Banville and I.R. Epstein, *J. Phys. Chem.* **85**, 2152 (1981).

[5] J.A. Pojman and I.R. Epstein, *J. Phys. Chem.* **95**, 1299 (1991).

[6] S. Dushman, *J. Phys. Chem.* **8**, 453 (1904).

[7] J.R. Roebuck, *J. Phys. Chem.* **6**, 365 (1902).

[8] J. Harrison and K. Showalter, *J. Phys. Chem.* **90**, 225 (1986).

[9] L. Forstova, H. Sevcikova, M. Marek and J. H. Merkin, *J. Phys. Chem. A* **104**, 9136 (2000).

[10] L. Forstova, H. Sevcikova and J. H. Merkin, *Phys. Chem. Chem. Phys.* **4**, 2236 (2002).

[11] M.R. Carrey, S.W. Morris and P. Kolodner, *Phys. Rev. E* **53**, 6012 (1996).

[12] M. Bockmann and S. Muller, *Phys. Rev. Lett.* **85** (12), 2506 (2000).

[13] D. Sharp, *Physica (Amsterdam) D* **12**, 3 (1984).

[14] K. Mikaelian, *Phys. Rev. E.,* **47**, 375 (1993).

[15] J.P. Keener and J.J. Tyson, *Physica (Amsterdam) D* **32**, 307 (1988).

[16] J. Martin, N. Rakotomalala, D. Salin and M. Bockmann, *Phys. Rev. E* **65**, 051605 (2002).

[17] J. Huang, D.A. Vasquez, B.F. Edwards and P. Kolodner, *Phys. Rev. E* **48**, 4378 (1993).

[18] B. F. Edwards, J.W. Wilder and K. Showalter, *Phys. Rev. A* **43**, 749 (1991).

[19] J.W. Wilder, D.A. Vasquez and B.F. Edwards, *Phys. Rev. E* **47**, 3761 (1993).

[20] J.W. Wilder, B.F. Edwards and D.A. Vasquez, *Phys. Rev. A* **45**, 2320 (1992).

[21] D.A. Vasquez, J.W. Wilder and B.F. Edwards, *Phys. Fluids A* **4**, 2410 (1992).

[22] J. Masere, D.A. Vasquez, B. F. Edwards, J.W. Wilder and K. Showalter, *J. Phys. Chem.* **98**, 6505 (1994).

[23] D. Rose, M. S. Thesis, University of Toronto, unpublished, (1997).

[24] I. Nagypal, G. Bazsa and I.R. Epstein, *J. Am. Chem.* **108**, 3635 (1986).

[25] H. Sevcikova and M. Marek, *Physica (Amsterdam) D* **13**, 379 (1984).

[26] B.F. Edwards, *Phys. Rev. Lett.* **89** (10), 104501 (2002).

[27] M. Leconte, J. Martin, N. Rakotomalala and D Salin, *Phys. Rev. Lett.* **90** (12), 128302 (2003).

[28] D.A. Skoog and D.M. West, "Analytical Chemistry", 3rd ed., Holt, Rinehart and Winston, New York (1979).

[29] A. Toth, V. Gaspar and K Showalter, *J. Phys. Chem.* **98**, 522 (1994).

[30] E. Kelley and M. Wu, *Phys. Rev. Lett.* **29**, 1265 (1997).

[31] M. Wu and M. Gharib, *Physics of Fluids*, **14** (7), L49 (2002).